Original Research Article

Density Functional Theory Study of the Effect of Mono-Halogen Substitution on Electronic and Non-Linear Optical Properties of Porphyrin

ABSTRACT

Porphyrin is an organic macrocycle compound, with a chemical formular (C20H14N4) it act as important components in various technological application like solar cell, due to their flexibility and low production cost. In this work, DFT and TD-DFT were used to investigate the molecular geometry, HOMO-LUMO energy gap, global chemical indices, thermodynamic properties, non-linear optical properties, IR frequencies and IR intensities, open circuit voltage and UV-Vis spectrum of parent and substituted porphyrin molecules were calculated and noted. All the computations were performed by using Gaussian 03 package. Our result for the bond lengths indicates that the strongest bond was found in chloroporphyrin molecule with value of 1.0771(Å) and the highest bond angles was found to be 130.93^0. The calculated value of HOMO-LUMO energy gap shows that porphyrin will be more stable by the substitution of fluoride atom with HOMO-LUMO energy gap of 5.5865eV. The value of energy gap for parent porphyrin molecule (2.8885) eV was found to be very closer to the reported value of (2.920) eV. It was found that the zero point vibrational energy reduces, while the entropy and specific heat capacity of the molecules rises, due to the effect of the substitutions. The non-linear optical properties calculations shows that, the first-order hyperpolarizability (β_{tot})values turn out to be ten times than that of the prototype urea ($0.3728\ x10^{-24}$ esu) molecule, which is commonly used for the comparison of NLO properties with other materials. The computed frequencies and intensities result shows that fluoroporphyrin has slightly higher peak values of frequencies with corresponding intensities than the rest of the substituted porphyrin molecules. The open circuit voltage ranges from 2.0206-4.1568eV in the case of high LUMO and 0.9465-3.0828eV in the case of low LUMO, this value can be applied to organic solar cell. The UV-VIS spectrum, shows that due to the solvent effect there was an increase in the excitation energy and then slight increase in oscillator strength. Our finding shows that the hybrid halogenated compound may be utilized as an application in sensor and solar cells.

KEYWORDS: Porphyrin, TD-DFT, entropy, dipole moment, softness

1.0 **INTRODUCTION**

Organic semiconductor materials have attracted the interest of some scientists in the world, due to their strong stability, peak carrier mobility and better efficiency in terms of lifetime manufacturing cost as well as the outcome performance of organic electronic materials such as organic thin film transistor (OTFTs), organic solar cell, photo-detectors, gas sensors and so on (Ziyang *et al*., 2020). These π-functional systems, have optoelectronic properties that land themselves in applications such as solar cells, sensors (Menke and Holmes, 2014), nanolasers (Wang *et al*., 2007), organic field-effect transistors (OFETs) (Gao *et al*., 2013; Beaujuge and Fréchet, 2011) and organic light-emitting diode (OLEDs) (kulkarni *et al*., 2004; Burroughes *et al*., 1990).

Porphyrins are tetrapyrolic macrocycles with π-conjugated electronic system that are common in nature and have various technological applications (Benkrima et al., 2022,2023). Porphyrin and its derivatives is widely studied compound that commonly exist in haemoglobin, chlorophyll and petroporphyrin (Ammar and Badran , 2019). Due to their huge π-conjugation, porphyrins have powerful absorption in UV and visible region forming coloured compound (Bhaskar *et al.*, 2020). In addition, the large π-conjugated system is responsible for many properties and show potential application in various fields (Kumer, 2017). Porphyrins and their derivatives have been studied using a range of computational approaches, according to literature review of theoretical modelling of Porphrins. A survey by Shubina (2020) recorded these computational strategies, which ranged from linear combination of atomic orbitals(LCAO), molecular mechanics, semi-empirical methods, through self-consistent field method (SCF)in the earlier literature, to the modern day methods which include molecular dynamics (MD), density functional theory (DFT), configuration interaction(CI), and coupled cluster (CC), methods. Among the numerous computationaltechniques utilized, recent literature is flooded with DFT calculations of molecular Porphyrin and its derivatives primarily to understand their frontier orbital configuration, electron occupancy, charge transfer, and excited state properties. The DFT functionals used to study the porphyrincomplexes include all the rungs of the "Jacob's Ladder" with variable approximations(Bhaskar et al, 2020).

In 2010,Leonardo et al, reported the investigation of theoretical study of structure and non-linear optical properties of Zn(II) porphyrin adsorbed on carbon nanotubes. The structure and stability of a series of porphyrin-nanotube complexes (Znp-SWNT, H_2 P-SWNT,ZnP-pp-SWNT and H_2 P-pp-SWNT) and first order hyperpolarizability were computed using DFT and a couple–perturbed-HF approach. The presence of Zn(II) contributes significantly to the complex stability, and push-pull substituents further enhance the stability. Porphyrin and SWNT interact through the potential energy surfaces, five stable arrangement (m1-m5) were found in the position of porphyrin ring along the tube axis. Intermolecular distances increased as porphyrin approached extremities of the tube (from m1-

m5), resulting in less durable complexes. TheH_2P-pp-SWNT and ZnP-pp-SWNT had highest first hyperpolarizability around 100×$10^{-30} esu^{-1} cm^5$. The adsoption on the tube surface raised the β value by ~40% compared to the free porphyrin H_2P-pp and ZnP-pp. Their result thus suggest the porphyrin SWNT nanocomposites may be consideredas a possible system for NLO application.

Moreover, Giovanelli et al (2017) reported the electronic structure of tetra(4-amino phenyl)porphyrin studied by photoemission, UV-Vis spectroscopy and density functional theory. By using direct and inverse photoemission as well as comparison to DFT computation, the valence and the conduction bands of thin films of tetra(4-amino phenyl) were examined. The measured electronic transport energy gap (E=1.85eV) between the highest occupied molecular orbital (HOMO) and lowest unoccupied molecular orbital (LUMO) in TAPP was found to reducesignificantlywith respect to TPP. Furthermore, the HOMO-LUMO electronic transport gap was shown to decrease with electron-donor amino functionalization, and the HOMO to HOMO-1 energy separation was observed to grow in a manner that is compatible with an orbital destabilizing process. These results, together with TD-DFT computations, were utilized to examine how the UV-Vis spectrum changed when an amino was substituted. This finding shows that photoemission could be used in addition to other tools to address the molecular optical problem.

In 2019, Ammar and Badran examined the effect of CO adsorption on properties of transition metal doped porphyrin based on DFT and TD-DFT study. They found that the structural, electronic and optical properties of transition metal doped porphyrin as well as the effect of CO-adsorption on TM@P. The P and TM@P; TM=Mn, Fe, Co, Ni, Cu, and Zn molecules are planar. and the CO molecule prefers to interconnected with P and TM@P through its carbon head. Thus, it is not advised to employ TM@P complexes as an electrochemical CO gas sensor. Certain TM-doped porphyrin (Mn@P, Co@P, Fe@p) are optically sensitive to CO gas according to the result of the TD-DFT calculation.

An interesting study was conducted by Badran et al. in 2021. They used DFT (Density Functional Theory) and TD-DFT (Time-Dependent Density Functional Theory) calculations to investigate the adsorption of halogen atoms (F, Cl, and Br) on cobalt-doped porphyrin (CoP). Additionally, they examined the influence of an external static electric field on the adsorption process and the UV-Vis spectra. One of the findings of the study was that the introduction of cobalt doping increased the stability of the porphyrin molecule. Moreover, it was observed that the HOMO-LUMO gap (Eg) of the system was widened to 3.11 eV as a result of the Co-doping. The HOMO-LUMO gap is an important parameter that determines the optical and electronic properties of a material. A wider HOMO-LUMO gap generally implies a higher energy required for electronic transitions, which can have implications for the absorption and emission spectra of the system.These results suggest that cobalt doping in

porphyrin systems can have a significant impact on their stability and electronic structure, which may be beneficial for applications in fields such as catalysis or optoelectronics. The study also highlights the importance of external electric fields in modulating the adsorption behavior and the optical properties of these systems.There is slightly increase in the dipole moment to 0.015 Debye and converts the porphyrin from optically UV active into visibly active material. The NBO atomic charges suggest that the halogen is interacted because of the charge transfer mechanism. In the investigated result of Badran *et al.*, UV-Vis is calculated but IR spectra, NLO and thermodynamic properties wee not reported.

This study focuses on investigating the effect of mono-halogen elements (specifically bromine, chlorine, and fluorine) on various properties of porphyrin molecules, including nonlinear optical (NLO) behaviour, thermodynamic characteristics, infrared (IR) spectra, and open circuit voltage. The parent and substituted halogenated porphyrin molecules considered in this research have not been previously documented in existing literature.

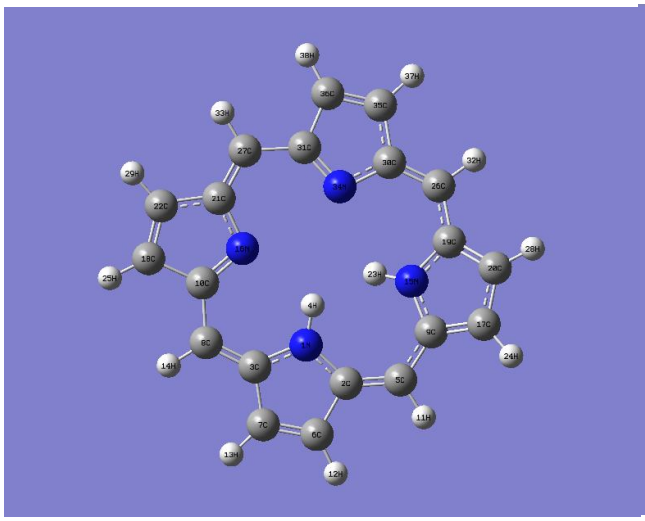

1a:Parent Porphyrin molecule

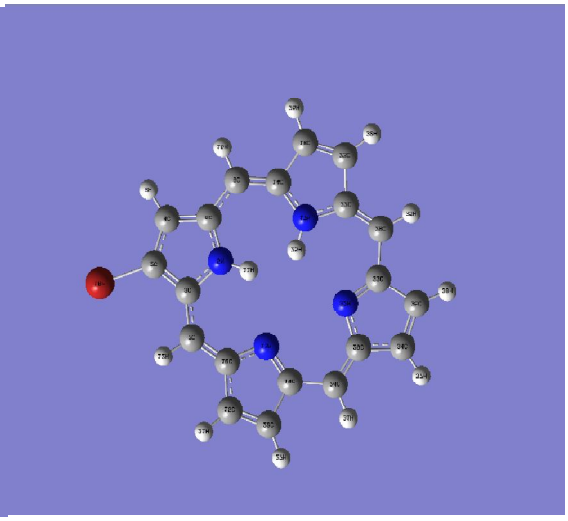

1b:Bromoporphyrin molecule

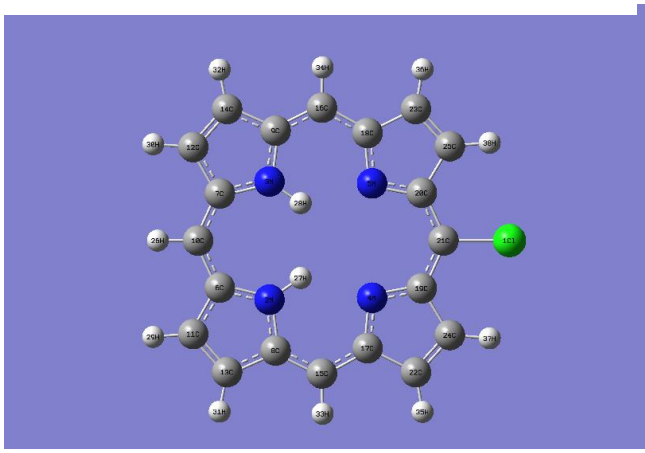

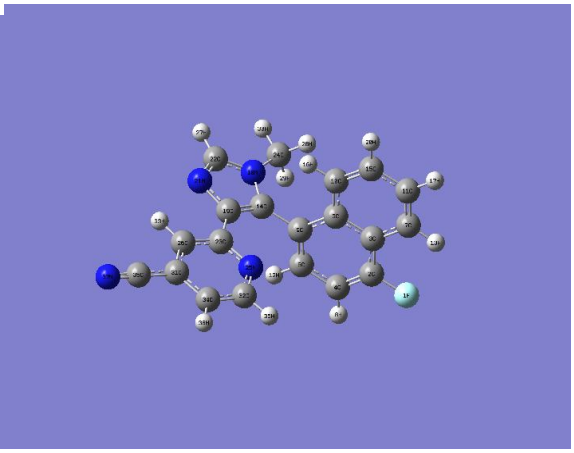

Figure1: Optimized structure of Parent Porphyrin and substituted porphyrin molecule

2.1 DENSITY FUNCTIONAL THEORY

Density functional theory (DFT) is a computational quantum mechanical modelling method used in physics, chemistry and materials science to investigate the electronic structure or nuclear structure (principally the ground state) of many-body systems, in particular atoms, molecules, and the condensed phases. Using this theory, the properties of a many-electron system can be determined by using functionals, i.e. functions of another function, which in this case is the spatially dependent electron density. Hence the name density functional theory comes from the use of functionals of the electron density. DFT is among the most popular and versatile methods available in condensed-matter physics, computational physics, and computational chemistry. DFT has been very popular for calculations in solid-state physics since the 1970s.

However, DFT was not considered accurate enough for calculations in quantum chemistry until the 1990s, when the approximations used in the theory were greatly refined to better model the exchange and correlation interactions. Computational costs are relatively low when compared to traditional methods.Although density functional theory has its roots in the Thomas–Fermi model for the electronic structure of materials, DFT was first put on a firm theoretical footing by Walter Kohn and Pierre Hohenberg in the framework of the two Hohenberg–Kohn theorems (H–K)(Hohenberg 1964). The original H–K theorems held only for nondegenerate ground states in the absence of a magnetic field, although they have since been generalized to encompass these (levy *et al*., 1979).

2.1 Global Chemical Reactivity Descriptors (GCRD)

Global reactivity descriptors such as chemical potential, chemical hardness-softness, electronegativity and electrophilicity index are useful quantities in predicting and understanding global chemical reactivity trends. The ionization potential (IP) and electron affinities (EA) of the studied molecules are computed by using Koopmansapproximation as (Roy, 2018):

$$IP = -E_{HOMO} \quad (1)$$

$$EA = -E_{LUMO} \quad (2)$$

The energy gap E_g can be obtained from the relation;

$$E_g = E_{LUMO} - E_{HOMO} \approx IP - EA \quad (3)$$

The chemical hardness (η) is expressed in terms of IP and EA by(Babaji *et al*., 2016);

$$\eta = (E_{LUMO} - E_{HOMO})/2 \approx (IP - EA)/2 \quad (4)$$

And softness is given by (Babaji *et al*., 2016);

$$s = \frac{1}{\eta} \quad (5)$$

The chemical potential is given by (Khan *et al*., 2017);

$$\mu = -(\frac{IP+EA}{2}) \quad (6)$$

The electronegativity is given by (Khan *et al*., 2017);

$$X = \frac{IP+EA}{2} \quad (7)$$

The electrophilictity index is a measure of energy lowering due to maximal electron flow between donor and acceptor. Electrophilictity index (ω) is expressed as (Khan *et al*., 2017; Srivastava *et al*., 2014);

$$\omega = \frac{\mu^2}{2\eta} \quad (8)$$

2.3 Non-Linear Optical Properties

In order to gain an insight into the study of non-linear optical properties (NLO) of porphyrin molecule; the dipole moment (μ), polarizability (α), anisotropic polarizability (Δα), and hyperpolarizability (β and γ) were computed at DFT/B3LYP using 6-311++G(d,p) basis set.

For molecular systems, dipole moment can be obtained from (Khan *et al*., 2017);

$$\mu_{tot} = [\mu_x^2 + \mu_y^2 + \mu_z^2]^{1/2} \quad (9)$$

Where μ_x, μ_y *and* μ_z are the components of dipole moment in x, y and z coordinates.

Electric dipole polarizability is given by (Haider *et al*., 2015);

$$\alpha = -\frac{\partial^2 E}{\partial F_a \partial F_b} \quad (10)$$

Where E is the electric field,F is the induced dipole moment, while a and b are coordinates of x, y and z.

The mean polarizability is calculated using (Khan *et al*., 2017);

$$< \alpha >= \frac{1}{3}\ (\alpha_{xx} + \alpha_{yy} + \alpha_{zz}) \qquad (11)$$

Where the α_{xx}, α_{yy} *and* α_{zz} quantities are known as principal values of polarizability tensor.

The anisotropic polarizability is given by (Khan *et al*., 2017);

$$\Delta\alpha = 2^{-1/2}[(\alpha_{xx} - \alpha_{yy})^2 + (\alpha_{yy} - \alpha_{zz})^2 + (\alpha_{zz} - \alpha_{xx})^2 + 6\alpha_{xx}^2]^{1/2} \qquad (12)$$

The first hyperpolarizability is defined as (Abdulaziz *et al*., 2019);

$$\beta = [(\beta_{xxx} + \beta_{xyy} + \beta_{xzz})^2 + (\beta_{yyy} + \beta_{yzz} + \beta_{yxx})^2 + (\beta_{zzz} + \beta_{zxx} + \beta_{zyy})^2]^{1/2} \qquad (13)$$

The second order hyperpolarizability is given by (Haider *et al*., 2015);

$$\gamma = \frac{1}{5}[\gamma_{xxxx} + \gamma_{yyyy} + \gamma_{zzzz} + 2(\gamma_{xxyy} + \gamma_{xxzz} + \gamma_{yyzz})] \qquad (14)$$

2.4 Open-Circuit Voltage (Voc)

The maximum open-circuit voltage (Voc) is an important characteristic that can be calculated theoretically by the difference between highest occupied molecular orbital (HOMO) and the lowest unoccupied moleculer orbital (LUMO). The value of Voc has been calculated from the expression (Shuwa et al., 2021)

$$V_{oc} = E_{Homo}^{Donor} - E_{Lumo}^{Acceptor} - 0.3 \qquad (15)$$

3.0 COMPUTATIONAL METHOD

The calculations in this study were conducted using Density Functional Theory (DFT) at the B3LYP level employing the 6-311++G (d, p) basis set (Chengteh and Weitao, 1988), The computational tool Gaussian 03 package (Frisch et al., 2004) was utilized for these calculations. All parameters were allowed to relax, resulting in optimized geometries that correspond to the minimum energy configurations. The optimization procedure was iteratively performed until a moderately low-energy geometry was achieved. The optimized geometries were further utilized to determine the energy values of the Highest Occupied Molecular Orbital (HUMO) and Lowest Unoccupied Molecular Orbital (LUMO), which allowed for the calculation of the energy band gap (Eg) and global chemical index parameters. Additionally, at the same level of theory, various molecular properties were computed using the same optimized geometries, including the total dipole moment (μ_{tot}), electric dipole polarizability (α), mean polarizability ($<\alpha>$), anisotropic polarizability ($\Delta\alpha$), hyperpolarizabilities (β and γ), entropy (S), and specific heat capacity (C_v) of the investigated molecules. Furthermore, the IR frequencies and force constants for all normal modes of the molecule were determined. In the calculation of IR spectra, the optimized molecule resulting from the geometry

optimization was used as the initial structure for frequency calculations. The frequencies were then computed based on the energy of the input structure, providing the spectra for the molecules. Finally, the obtained spectra were interpreted using IRPal 2.0 version software.

4.0 RESULTS AND DISCUSSION

4.1 Optimized Parameters

The bond length is the measurable distance joining two atoms covalently bonded together. The smaller the bond lengths the higher the bond energy (Suzuki *et al.*, 2006).Selected values of bond lengths and bond angles of the studied moleculesare listed in Tables 1a-c. The result shows that the lowest value obtained was 1.0771(Å) in chloroporphyrin molecule. Although, when compared with the results of the parent molecule, the bond lengths in chloroporphyrin molecule tends to be a little smaller which suggests that chloroporphyrin has the strongest bond energy than the rest of the substituted mono halogen molecules.

The bond angle is the mid-point angle joining the orbitals of the central atom containing the bonding electron pairs in the molecule, expressed in degrees (Mason and Brady, 2007). From Table 1b, the results of the substituted molecules show some small changes in the bond lengths.Likewise from Table 1c, the substitution of halogen atoms shows a slight increment in the bond angles of the studied molecules. From the results, the values obtained in chloroporphyrinare a bit higher than the one obtained in the other substituted molecules.

Table 1a: Selected Bond Lengths (Å) and Bond angles of the Optimized Structure of Parent Porphyrin molecule using B3LYP/ 6-311++G (d, p) Basis Sets.

Bond Lengths (Å)		Bond Angle(˚)	
R(1,2)	1.3731	A(1,2,6)	106.2606
R(2,6)	1.4365	A(2,1,3)	110.6293
R(8,14)	1.0835	A(3,1,4)	117.3793
R(10,18)	1.4577	A(9,5,11)	114.4880
R(20,28)	1.0794	A(30,26,32)	118.5421

Table 1b: Selected Bond Lengths (Å) of the Optimized Structure of Substituted Porphyrin Molecules.

Bond Lengths (Å)	Bromoporphyrin	Chloroporphyrin	Bond lengths(Å)	Fluoroporphyrin
R(2,6)	1.3730	1.3734	R(2,6)	1.3851
R(2,8)	1.3780	1.3763	R(7,11)	1.3791

R(4,17)	1.3598	1.3606	R(10,18)	1.4181
R(12,14)	1.3700	1.3701	R(15,21)	1.4040
R(24,37)	1.0809	1.0771	R(23,37)	1.0863

Table 1c: Selected Bond Angles (˚) of the Optimized Structure of SubstitutedPorphyrin Molecule

BondAngles(˚)	Bromoporphyrin	Chloroporphyrin	BondAngles(˚)	Fluoroporphyrin
A(6,2,8)	111.0252	110.5185	A(6,2,12)	107.0791
A(8,2,27)	116.8602	117.7339	A(10,8,13)	117.8508
A(17,4,19)	106.2362	105.9617	A(18,20,19)	120.2206
A(13,8,15)	130.5345	129.7984	A(24,23,37)	120.0117
A(19,21,20)	130.5434	130.9380	A(30,17,32)	109.0511

4.2 Frontier Molecular Orbital

The values of the HOMO-LUMOenergy gap of the parent and substituted Porphyrin are presented in Table 2. It is revealed that, compounds with higher HOMO-LUMO energy gap tend to be more stable than the one with lower energy band gap (Srivastava *et al.*, 2014). And also, the lower the energy band gap,the easier for an electron to be emitted to the ground state(Hasan, 2013).The results obtained in Table 2 show that fluoroporphyrin has the highest value of energy band gap of about 5.5865eV,follow by chloroporphyrin and then bromoporphyrin molecule with 4.1037eV and 3.9563eV respectively.This shows that fluoroporphyrin molecule has highest kinetic stability than the other substituted molecules.The result obtained for energy band gap in theparent molecule(2.88eV)was found to be in agreement with theoretical and experimental values of 2.9eV (Badran *et al.,* 2021).

Table 2: Calculated HOMO, LUMO, Energy gap in (eV), Ionization Potential and Electron Affinity of the Optimized Structure of substituted porphyrin Molecules

Molecules	IP (e V)	EA (eV)	E_{HOMO}(eV)	E_{LUMO} (eV)	E_{gap} (eV)	Previous work (Badran*et al., 2021*)
Parentporphyrin	5.5465	2.6580	-5.5465	-2.6580	2.8885	2.920
Bromoporphyrin	6.7713	2.8150	-6.7713	-2.8150	3.9563	
Chloroporphyrin	6.9043	2.8005	-6.9043	-2.8005	4.1037	

Fluoroporphyrin	7.6828	2.0963	-7.6828	-2.0963	5.5865	

TheIonization potential (IP) and electron affinity (EA) are important parameters that can be determined to acquire or release an electron (Kumer *et al.,* 2017). The IPs and EAs are also presented in Table 2. From the results obtained, it is observed thatfluoroporphyrin has thehighest value of ionization potential as well as lowest value of electron affinitiesthanthe other substituted Porphyrin molecules.

4.3 Global Chemical Reactivity Descriptors (GCRD)

GCR parameters of molecules (that ishardness (η), softness (ʃ), chemical potential (μ), electronegativity (χ) and electrophilicity index (ω)) of the parent Porphyrin and its substituted molecules are reported in Tables 3 using molecular orbital energy. Chemical hardness is said to increase with the increase in the HOMO-LUMO energy gap. A molecule with higher chemical hardness is said to be more stable and less reactive. As seen in Table 3,fluoroporphyrin with a slightly higher value of chemical hardness of 2.7932 eV is considered to be harder and more stable than the rest of the substituted molecules, followed by chloroporphyrin and then bromoporphyrin with chemical hardness 2.0519 eV and 1.9781eV respectively.

Table 3: Global Chemical Indices of the Optimized Structure of the SubstitutedPorphyrin Molecules

Molecules	$\boldsymbol{\eta\,(eV)}$	$\boldsymbol{\int(eV)}$	$\boldsymbol{X(eV)}$	$\boldsymbol{\mu(eV)}$	$\boldsymbol{\omega(eV)}$
Parent porphyrin	1.4442	0.6924	4.1022	-4.1022	5.8260
Bromoporphyrin	1.9781	0.5055	4.7931	-4.7931	5.8070
Chloroporphyrin	2.0519	0.4873	4.8524	-4.8524	5.7375
Fluoroporphyrin	2.7932	0.3580	4.8895	-4.8895	4.2795

4.4 Thermodynamic Properties

The thermodynamic parameters presented in Tables 4 such as predicted total energy (E), electronic, translational, rotational, vibrational, zero-point vibrational energy (ZPVE), entropy (S), molar heat

capacity (C_V), and rotational constant for both parent and substituted porphyrin molecules were calculated at constant temperature and pressure of about 298.1K and 1atm respectively. The analysis of thermodynamic parameters is important to predict the outcome of a chemical reaction. Our findings show that substitution offluorine improves the molar heat capacity (C_V),entropy (S) and zero-point vibrational energy (ZPVE)of the Porphyrinthan the other substituted molecules.By analysing the results obtained the variation of thermodynamic properties changes slightly due to the effect of the substitutions. Therefore, we conclude that the substitutions have influence on the thermodynamic properties of the molecules. The results affirm that these substituted molecules have high chemical reactivity and thermal resistivity than the parent Porphyrin due to the increase in their kinetic energy.

Table 4: Thermodynamic properties of the optimized structure of parent porphyrin and substituted porphyrin molecules

Molecules	**Parentporphyrin**		**Bromoporphyrin**		**Chloroporphyrin**		**Flouroporphyrin**	
Position	**Cv**	**S**	**Cv**	**S**	**Cv**	**S**	**Cv**	**S**
Electronic	0	0	0	0	0	0	0	0
Translational	2.981	42.474	2.981	43.760	2.981	43.401	2.981	43.260
Rotational	2.981	33.241	2.981	36.056	2.981	35.351	2.981	35.184
Vibrational	65.930	37.351	70.146	60.531	69.900	58.981	71.181	72.925
Total	71.892	130.264	76.107	140.347	75.861	137.734	77.143	151.368
Rotational constants (GHz)	0.2787, 0.13238	0.25216,	0.27264, 0.08211	0.11749,	0.25358, 0.10947	0.19263,	0.35468, 0.12495	0.14284,
ZPVE(Kcal/Mol)	184.20397		177.82499		178.20885		178.73674	

4.5 Non-Linear Optical Properties

As NLO active materials find applications in telecommunications, and potential applications in modern technologies, Non-linear optics plays a key role in the current demand in global research. To understand the relationships between molecular structure and nonlinear optical properties, the mean, anisotropic, first and second-order hyperpolarizabilities of Porphyrin and its substituted molecules were calculated andpresented in Table 5.

It was observed that, there is an increase in the values of total dipole moments (μ_{tot}) due to the present of the substitutions. The total dipole moment, (α_{tot}) of the substituted molecules increases in the

order of bromoporphyrin<chloroporphyrin<fluoroporphyrin. The significant increase in the dipole moments of the substituted molecules leads to our belief that they are polar materials.From the result obtainedfor the first order hyperpolarizability in Table 5, it was found that the value of fluoroporphyrin molecule (3.6605×10^{-30}) is about ten times than that of the prototype urea. However, substituting the parent molecule with halogen atoms (bromine, chlorine and fluorine) we realized that its first-order hyperpolarizability (β) values turn out to be larger than that of the prototype urea (0.3728 x10^{-30} esu), which is commonly used for the comparison of NLO properties with other materials. Given the foregoing, we conclude that substitution of Porphyrin with halogens placed it in another field of application in the linear and nonlinear optics. This implies that the presence of the substitutions improved the NLO properties under study.

Table 5: Non-Linear Optical Properties of Parent and Substituted Porphyrin molecules

Parameters	Porphyrin	Bromoporphyrin	Chloroporphyrin	Fluoroporphyrin
μ_{tot} (Debye)	2.2642	2.2711	4.3485	6.5795
$\langle\alpha_{tot}\rangle \times 10^{-24}$esu	18.7706	21.6926	20.6421	22.2280
$\langle\Delta\alpha\rangle \times 10^{-24}$esu	13.0331	36.7094	34.8168	58.4567
$\beta_{tot} \times 10^{-30}$esu	0.0958	1.5515	0.7197	3.6605
$\gamma_{tot} \times 10^{-36}$esu	1.5099	2.1953	1.9962	2.2686

4.6 Open circuit voltage (V_{oc})

The differences between the HOMO and the LUMO of the electron determines the open-circuit voltage of an organic solar cell, taking into account the energy lost during the production of photo charges (Kumer, 2017). The value of open-circuit voltage has been calculated using equation (15). In addition, low LUMO of the π-conjugated compounds and a high LUMO of the acceptor of the electron (PC71BM, PC61BM) increase the value of V_{oc}, which contributes a high efficiency of the solar cells (Maria et. al., 2019). The theoretical values of the open circuit voltage Voc of the studied molecules range from 2.0206to 4.1568 eV in the case of PC61BM and 0.9465 to 3.0828eV in the case of PC71BM as shown in Table 6. These values are sufficient for a possible efficient electron injection into LUMO of the acceptor.

Table 6: Calculated values of Open Circuit Voltage (V_{oc})

Molecule	E_{HOMO}(eV)	E_{LUMO}(eV)	V_{oc}(eV) $PC_{61}BM$	V_{oc}(eV) $PC_{71}BM$
Porphyrin	-5.5465	-2.6580	2.0206	0.9465
Bromoporphyrin	-6.7713	-2.8150	3.2453	2.1713
Chloroporphyrin	-6.9043	-2.8005	3.3783	2.3043
Fluoroporphyrin	-7.6828	-2.0963	4.1568	3.0828
$PC_{61}BM$ (Bourass et al., 2016)	−5.985	−3.226	******	******
$PC_{71}BM$ (Bourass et al., 2016)	−6.000	−4.300	******	******

4.7 IR Intensities

The main idea of frequency analysis is to get vibrational modes attached with precise molecular structures of the studied compound (Hamm *et al.,* 1998). Fig. 2shows the graphical representation of the calculated vibrational frequencies and intensities of the Porphyrin and substituted halogen molecules. The graphs show that there is a slight increase in the peak values of frequencies for the titled molecule due to the effect of the substitutions. From the graphs, the most intense frequency for bromoporphyrin is 3338.8617 cm^{-1} with corresponding intensities of 145.4988 km/mol. At this frequency, S (broad) dimer OH, W-NH stretch, S broad and Ar O-H bondedwere observed.For chloroporphyrin the most intense frequency is 812.4277 cm^{-1} with corresponding intensities of 161.9785 km/mol. At this frequency, S=CH out of plane,S,C-CL stretch, M,C-H out of plane, S (broad) and N-H wag amineswas observed.While, for fluoroporphyrin, the most intense frequency is at1628.7166cm^{-1} with corresponding intensities of 163.4209 km/mol. At this frequency, S,N-H out of plane, S, NH2 in plane bend, S, Ar-CH = CH-R and C=N were observed. Comparing the graphs presented, chloroporphyrin has slightly higher peak values of frequencies with corresponding intensities than the rest of the molecules. IRPAL 2.0 was used to interpret these frequencies(Wolf, 2010).

4.8 UV-Visible spectrum

UV-Vis spectrum is due to the reflectance spectroscopy in part of the ultraviolet, adjacent to the visible regions of the electromagnetic spectrum.It serves as the foundation for analysing various

compounds such as organic,inorganic and bio-molecules. How a new material absorbs energy in relation to the solar spectrum is a crucial consideration for use in photovoltaic materials (Shuwa et al, 2021). In this study, the UV-Vis spectrum was calculated from the optimized geometry of the studied molecule using TD-DFT at the B3LYP/6-311++G(d,p) level of theory.The UV - Vis spectrum was presented as oscillator strength against excitation energy as shown in Figures 3(a) and 3(b), Gaussview5.0 was used to plot the spectrum. Thetransition state, wavelength, excitation energy and oscillation strength are listed in Table 7 using four different solvents: Methanol, Chloroform, Toluene and Chlorobenzene. The result shows that due to the solvent effect there was an increase in the excitation energy and then slight increase in oscillator strength. The excitation energy was in the range of *2.2914-3.2525nm*while the oscillator strength was found tobewithin *0.0014-1.0279* in parent molecule, likewise in the halogen molecules, methanol was found to have the highest excitation energy in a halogens molecule while toluene has the highest excitation energy in parent molecule. It was observed that the lowest value of the excitation energy gives highest value of wave length.

Table 7: Wavelength (nm), Excitation energy (eV) and Oscillator strength of Bromoporphyrin and chloroporphyrin molecule

Solvent	Transition state	Bromoporphyrin			Chloroporphyrin		
		Wavelength λ (nm)	Excitation energy(eV)	Oscillator strength	Wavelength λ (nm)	Excitation energy (eV)	Oscillator strength
Chloroform	$S_0 \rightarrow S_1$	531.34	2.3334	0.1603	553.45	2.2402	0.1962
	$S_0 \rightarrow S_2$	490.68	2.5268	0.0048	504.81	2.4561	0.0094
	$S_0 \rightarrow S_3$	400.12	3.0987	0.0459	401.62	3.0871	0.5007
Chlorobenzene	$S_0 \rightarrow S_1$	532.49	2.3284	0.1722	554.97	2.2341	0.2096
	$S_0 \rightarrow S_2$	490.93	2.5255	0.0049	505.17	2.4543	0.0101
	$S_0 \rightarrow S_3$	399.59	3.1028	0.0674	402.79	3.0782	0.5815
Methanol	$S_0 \rightarrow S_1$	529.75	2.3404	0.1475	551.79	2.2469	0.1822
	$S_0 \rightarrow S_2$	490.35	2.5285	0.0048	504.80	2.4561	0.0077
	$S_0 \rightarrow S_3$	395.64	3.1337	0.0401	397.53	3.1189	0.4780
Toluene	$S_0 \rightarrow S_1$	531.72	2.5262	0.1634	553.67	2.2393	0.1992
	$S_0 \rightarrow S_2$	490.80	2.5262	0.0047	504.60	2.4571	0.0104
	$S_0 \rightarrow S_3$	403.19	3.0751	0.0430	403.87	3.0699	0.4743

Table 8: Wavelength (nm), Excitation energy (eV) and Oscillator strength of Porphyrin and Fluoroporphyrin molecule

Solvent	Transition state	Porphyrin			Fluoroporphyrin		
		Wavelength λ (nm)	Excitation energy(eV)	Oscillator strength	Wavelength λ (nm)	Excitation energy (eV)	Oscillator strength
Chloroform	$S_0 \rightarrow S_1$	531.34	2.3334	0.1603	368.06	3.3686	0.0271
	$S_0 \rightarrow S_2$	490.68	2.5268	0.0048	355.22	3.4904	0.0698
	$S_0 \rightarrow S_3$	400.12	3.0987	0.0459	319.93	3.8754	0.0080
Chlorobenzene	$S_0 \rightarrow S_1$	538.22	2.3036	0.0018	369.04	3.3596	0.0280
	$S_0 \rightarrow S_2$	520.22	2.3833	0.0025	355.95	3.4832	0.0723
	$S_0 \rightarrow S_3$	390.32	3.1765	1.0279	319.70	3.8781	0.0079
Methanol	$S_0 \rightarrow S_1$	534.65	2.3190	0.0014	373.50	3.3195	0.0241
	$S_0 \rightarrow S_2$	518.75	2.3900	0.0022	358.89	3.4546	0.0652
	$S_0 \rightarrow S_3$	381.20	3.2525	0.8912	319.00	3.8867	0.0057
Toluene	$S_0 \rightarrow S_1$	541.07	2.2914	0.0015	362.04	3.4246	0.0300
	$S_0 \rightarrow S_2$	520.98	2.3798	0.0024	351.39	3.5284	0.0710
	$S_0 \rightarrow S_3$	391.79	3.1645	0.9512	321.07	3.8616	0.0113

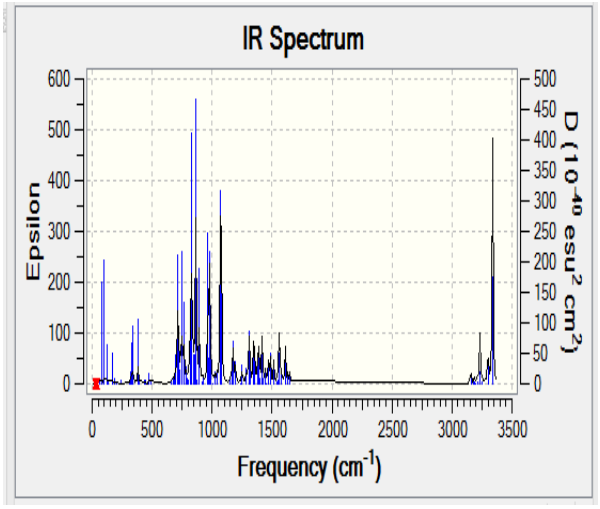

2a:Bromoporphyrin

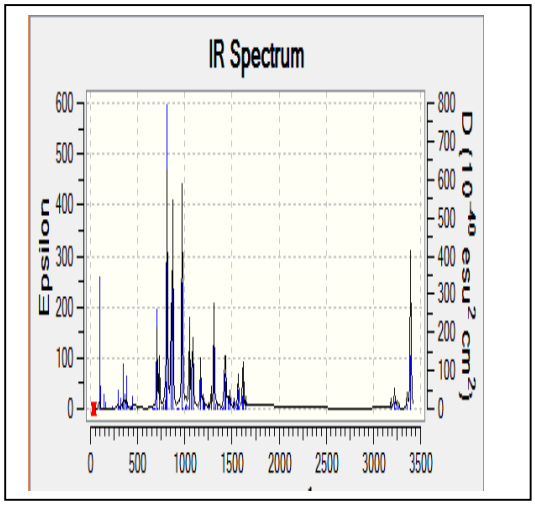

2b:Chloroporphyrin

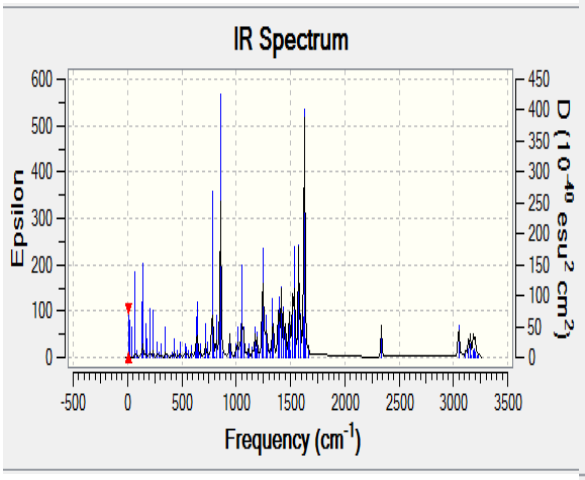

2c:Fluoroporphyrin

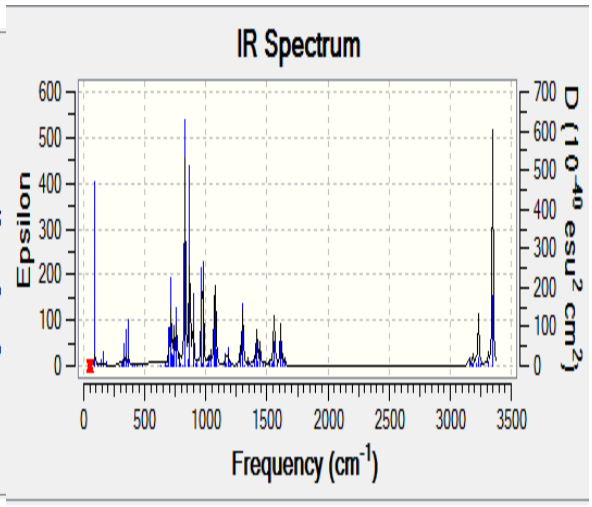

2d:Parent Porphyrin

Figure 2: Computed IR Spectra of porphyrin molecule

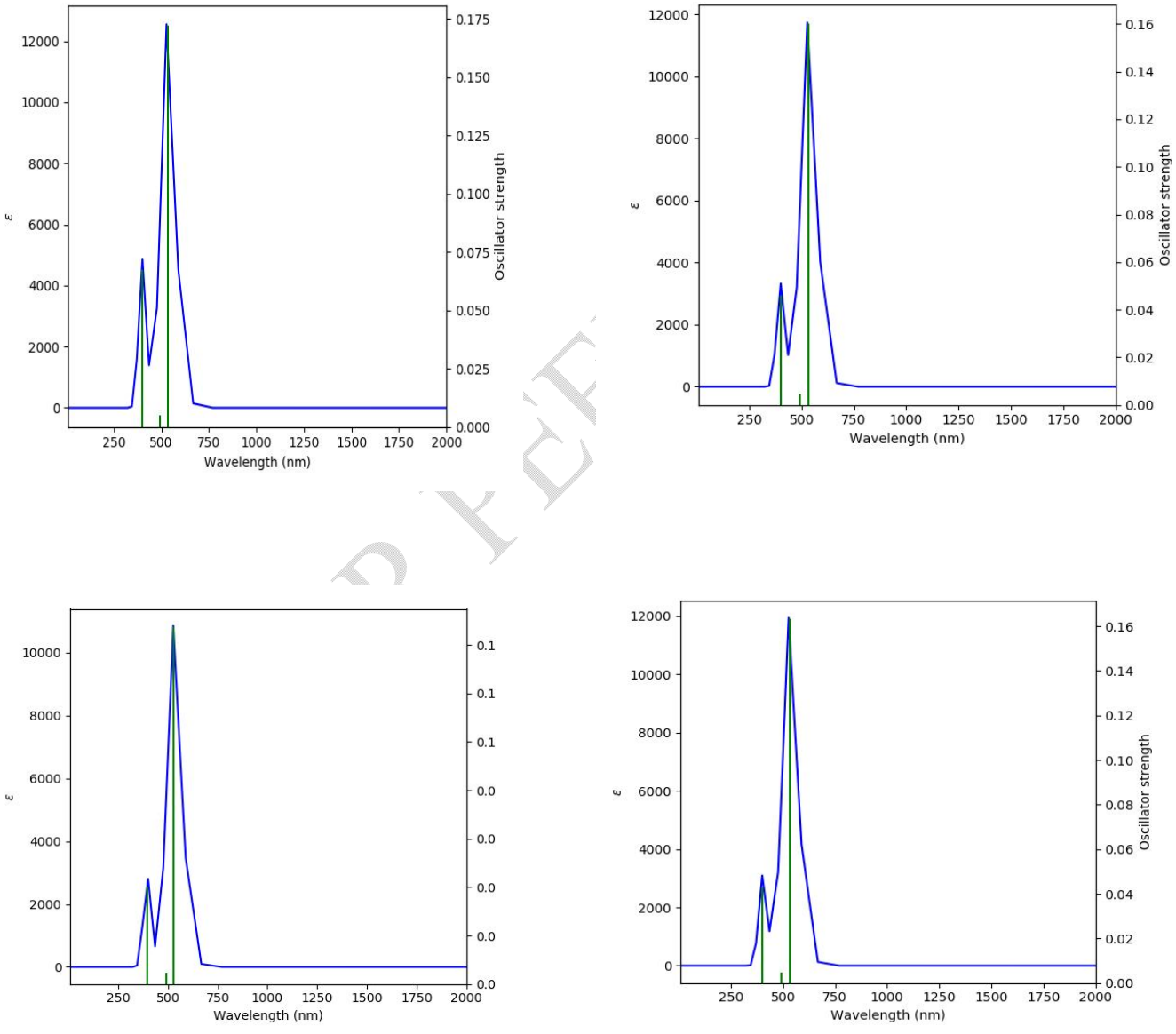

Figure 3(a): UV-Visible Spectrum of Porphyrin in solvents

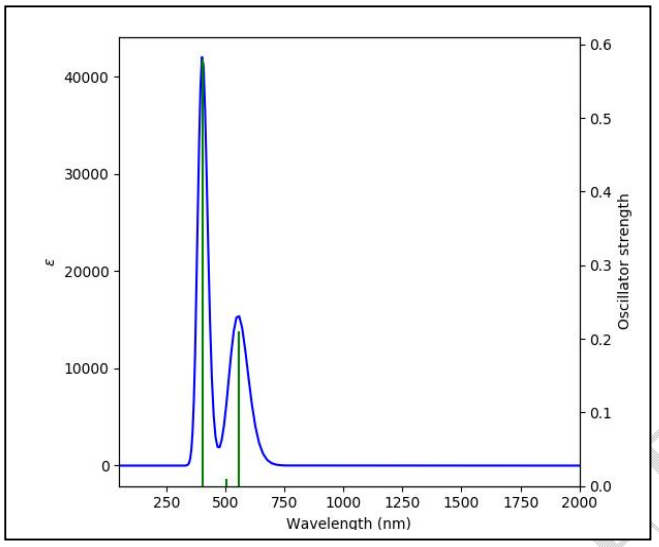

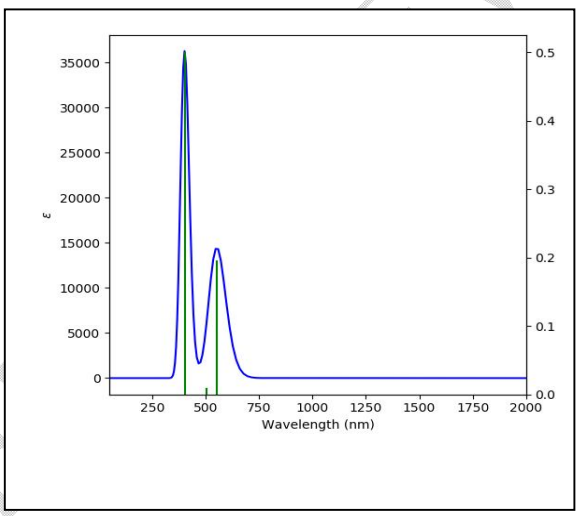

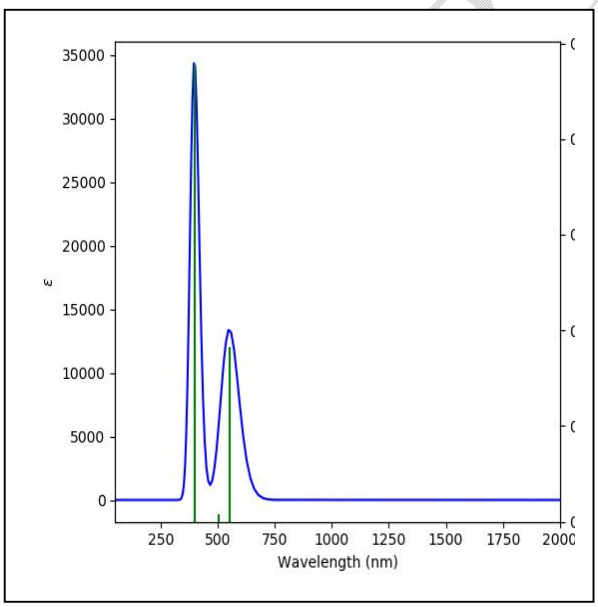

Methanol

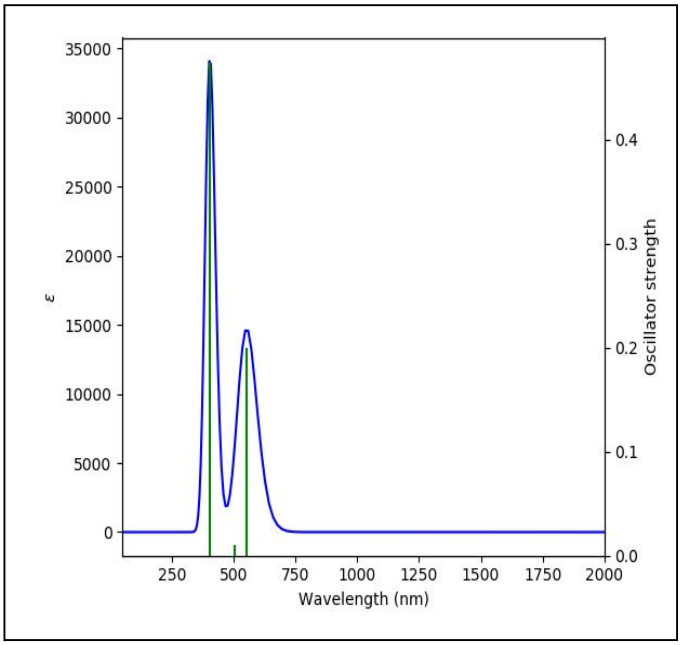

Toluene

Figure 3(b): UV-Visible Spectrum of Chloroporphyrin Molecules

5. CONCLUSION

In conclusion, our study investigated the optimized parameters, electronic properties, thermodynamic parameters, non-linear optical properties, and vibrational frequencies of parent porphyrin and its substituted molecules, with a focus on the effect of halogen atom substitution (bromine, chlorine, and fluorine) on the structure of porphyrin. The results obtained revealed that the substitution of fluorine in the titled molecule enhances the strength of its bond energy. Calculations of the HOMO-LUMO energy gap demonstrated that the substitution of fluorine atom increased the stability of porphyrin. Additionally, the thermodynamic properties indicated that the substitution improved the chemical reactivity and thermal resistivity of the molecule. In terms of frequencies and intensities, the chloroporphyrin molecule exhibited the most intense frequency at 812.4277 cm^(-1). Furthermore, the NLO results showed that halogen atoms (bromine, chlorine, and fluorine) displayed interesting properties such as high dipole moments and first-order hyperpolarizability (β). Notably, the open circuit voltage was determined to be 3.1885 eV, making it suitable for application in organic solar cells. The UV-VIS spectrum revealed excitation energies ranging from 529.75 eV to 532.49 eV and from 551.79 eV to 554.97 eV, while the corresponding oscillator strengths ranges from 0.1475 to 0.1722 and from 0.1822 to 0.2096. Overall, our findings suggest that the substituted molecules hold promise for applications in NLO materials, renewable energy, and emerging technologies.

REFRENCES

Abdulaziz H., Gidado A. S., Musa A., and Lawal. "Electronic structure and non-linear optical properties of neutral and ionic pyrene and its derivatives based on density functional theory". *JMater. Sci. Rev. 2(3), **2019**, 1-13*

Ammar H.Y, Badran H.M. Effect of CO adsorption on properties of transition metal doped porphyrin: A DFT and TD-DFT study. https://doi.org/10.1016/j.heliyon.2019.e02545
Appl. Sci. **2019**, *10*, 740; doi:10.3390/app10030740

Babaji G, Gidado AS, Abdulbaki MA. Determination of molecular structure, electronic and non-optical properties of hydralazine molecule. Transaction of the Nigerian Association of Mathematical Physics (NAMP). 2016;2:35- 48.

Badran H.M., Ammar H.Y., Kh.M. Eid, DFT and TD-DFT studies of halogens adsorption on cobalt-doped porphyrin:Effect of the external electric field.https://doi.org/10.1016/j.rinp.2021.103964

Beaujuge PM, Fréchet JM. Molecular design and ordering effects in π functional materials for transistor and solar cell applications. J. Am. Chem. Soc. 2011;33(50):20009–20029.

Bhaskar Chilukuri *, Ursula Mazur and K. W. Hipp Structure, Properties, and Reactivity of Porphyrins onSurfaces and Nanostructures with Periodic DFT Calculations. *Appl. Sci.2020, 10 740;* doi:10.3390/app10030740

Burroughes J, Bradley D, Brown A, Marks R, Mackay K, Friend R, Burns P, Holmes A. Light‐emitting diodes based on conjugated polymers. Nature. 1990 ;347(6293):539–54.

Chengteh Lee R. G. P. and Weitao Yang. **(1988**). "Developmenet of the Collesalvetti Correlation-Energy Formula into a Functional of the Electron Density". Phys. Rev. B. 37(2): 785–789.

Frisch M. J. H. M., Trucks G. W., Schlegel H. B., Scuseria G. E., Robb M. A., Cheeseman J. R., Scalmani G., Barone V., Mennucci B., Petersson G. A., Nakatsuji H., Caricato M., Li X., Hratchian P. H., lzmaylov A. F., Bloino J., Zheng G. and Sonnenberg J. L. (**2004).** Gaussian Software. Gaussian, INC.

Gao Y, Ding H, Wang H, Yan D. Electronic structure of interfaces between copper‐hexadecafluoro‐phthalocyanine and 2,5‐bis(4‐bipheny‐ lyl) bithiophene. Appl. Phys. Lett. 2007;91(14):142112.

Gioanelli L., Lee H.-L., Lacaze-Dufaure C., Koudia M., Clair S., Lin Y.-P.,Ksari Y., Themlin J.-M., Abel M., Cafolla A.A., "Electronic structure of tetra (4-aminophenyl)porphyrin studied by photoemission,UV-Vis spectroscopy and density functional theory" (2017) Journal of electron spectroscopy and related phenomena, Vol.218.pp.40-45.

Haider Abbas., Mohd Shkir., and AlFaify S. "Density Functional of spectroscopy, electronic structure, linear and non-linear optical properties of L-proline lithium chloride and L-proline lithium bromide monohydrate: For laser applications". *Phys. Sci. int. J.***2015**(12) pp. 2342-2344.

Hamm, P., Lim, M. and Hochstrasser R. M. (**1998).** "Structure of the amide 1 bond of peptides measured by Femtosecond nonlinear-infrared spectroscopy". *J. Phys. Chem.* B 102 (31): pp 6123

Hasan, N. B. (2013). Theoritical study of electronic properties of some Aromatic Rings: B3LYP/DFT Calculations. Advances in Physics Theories and Application,24, 83-92.

Hohenberg, pierre; Walter, Kohn (1964)."Inhomogeneous electron gas "Physical Review. 136 (3B):B864-B871.Bibcode:1964phRv..136..864H. doi:10.1103/physRev.136.B864.

Khan M. F., Bin Rashid R., Hossain A. and Rashid M. A. "Computational study of solvation free energy, dipole moment, polarizability, hyperpolarizability and molecular properties of botulin, a constituent of Corypha taliera (Roxb.)". *Dhaka Univ. J. Pharm. Sci. 16(1), **2017**, 1-8.*

Kulkarni AP, Tonzola CJ, Babel A, Jenekhe SA. Electron transport materials for organic light‐emitting diodes. Chem. Mater. 2004;16(23):4556–4573.

Kumer A., Ahmed B., Sharif A. and Al-mamun A. (**2017**) "A theoretical study of aniline and nitrobenzene by computational overview". *Asian J. Phys. Chem. Sci.* 4(2):1-12.

Leonardo A. Souza De., Antonio M.Da Silva Jr.,Georgia M.A Junqueira, Claudia Ana M. Carvalho, Helio F. Dos Santos. "Theoretical study of structure and non-linear optical properties of Zn(II) porphyrin adsorbed on carbon nanotubes".j.theochem.2010.08.018.

Levy, mel (1979).2universal variational functionals of electron densities, first order density matrices,and natural spin-orbitals and solution of the v-representability problem". Proceeding of the national Academy of sciences.76(12):60626065. Bibcode:1979NAS…76.6062L.doi:10.1073/pnas.76.12.6062.PMC411802.PMID16592733.

Maria A. Izquierdo,, Ria Broer,and Remco W. A. Havenith (2019) " Theoretical Study of the Charge Transfer Exciton Binding Energy in Semiconductor Materials for Polymer:Fullerene-Based Bulk

Heterojunction Solar Cells" J. Phys. Chem. A 2019, 123, 1233−1242
doi:https://pubs.acs.org/doi/10.1021/acs.jpca.8b12292

Mason P. E. and Brady J. W. **(2007).** "Tetrahedrality and the Relationship between Collective Structure and Radial Distribution Functions in Liquid Water". *J. Phys. Chem.* Vol. 111 (20): pp. 5669–5679.

Menke SM, Holmes RJ. "Exciton diffusion in organic photovoltaic cells". Energy Environ. Sci. 2014;(7):499–512.

Roy D.R, E.V. Shah, S.M. Roy, Optical activity of Co-porphyrin in the light of IR and Raman spectroscopy: a critical DFT investigation, Spectrochim. Acta A Mol. Biomol. Spectrosc. 190 (2018) 121–128.

Shuwa H.M, Mansur S, Gidado A.S, "Study of Electronic and molecular Properties of Poly(3-Octaylthiophene-2,5 diyl)Polymer Using Density Functional Theory (DFT) And Time Dependant Density Functional Theory(TD-DFT)".JMSRR,8(2): 41-52, 2021.

Srivastava K.K, Srivastava S, Alam T. Theoretical study of the effects of solvents on the ground state of TCNQ. Pelagia Res. Libr. 2014;5(1):288–295.

Suzuki S., Morita Y., Fukui K., Sato K., Shiomi D. T. and Nakasuji K. (**2006).** "Aromaticity on the pancake-bonded Dimer of Neutral phenalenyl Radical as studied by MS and NMR Spectroscopies and NICS Analysis" *J. Am. Chem. Soc.* 128 (8): 2530-2531.

Wang H, Xie Z, Ma Y, Shen J. Progress on the optoelectronic functional organic crystals. Sci. China Ser. B. 2007;50(4):433–452.

Wolf VH IR PAL V2.0, A table driving infrared Application; 2010. Available:Bhttp://home.kpn.nl/vheeswijk

Ziyang Zhang a, Zhengran He B, Sheng Bi C , Kyeiwaa Asare-Yeboah (2020).Phase segregation controlled semiconductor crystallization for organic thin film transistors. https://doi.org/10.1016/j.jsamd.2020.05.004

Y. Benkrima, M.E. Soudani, D. Belfennache, H. Bouguettaia, A. Souigat, Journal of Ovonic Research. Vol. 18, No. 6, November - December 2022, p. 797 – 804.

Y. Benkrima, S. Benhamida , D. Belfennache, Digest Journal of Nanomaterials and Biostructures. Vol. 18, No. 1, January - March 2023, p. 11- 19.